

Supporting Information

Increased Performance Improvement of Lithium-Ion Batteries by Dry Powder Coating of High-Nickel NMC with Nanostructured Fumed Ternary Lithium Metal Oxides

*Marcel J. Herzog, Nicolas Gauquelin, Daniel Esken, Johan Verbeeck, Jürgen Janek**

M. J. Herzog, Prof. J. Janek,
Institute of Physical Chemistry & Center for Materials Research Justus-Liebig-University
Giessen, Heinrich-Buff-Ring 17, 35392 Giessen, Germany
E-mail: Juergen.Janek@phys.Chemie.uni-giessen.de

Dr. N. Gauquelin, Prof. J. Verbeeck
Electron Microscopy for Materials Science, University of Antwerp, Campus Groenenborger,
Groenenborgerlaan 171, 2020 Antwerpen, Belgium and NANOlabor Center of Excellence,
University of Antwerp, 2020 Antwerpen, Belgium

M. J. Herzog, Dr. D. Esken
Evonik Operations GmbH, Rodenbacher Chaussee 4, 63457 Hanau-Wolfgang, Germany

Supporting Information

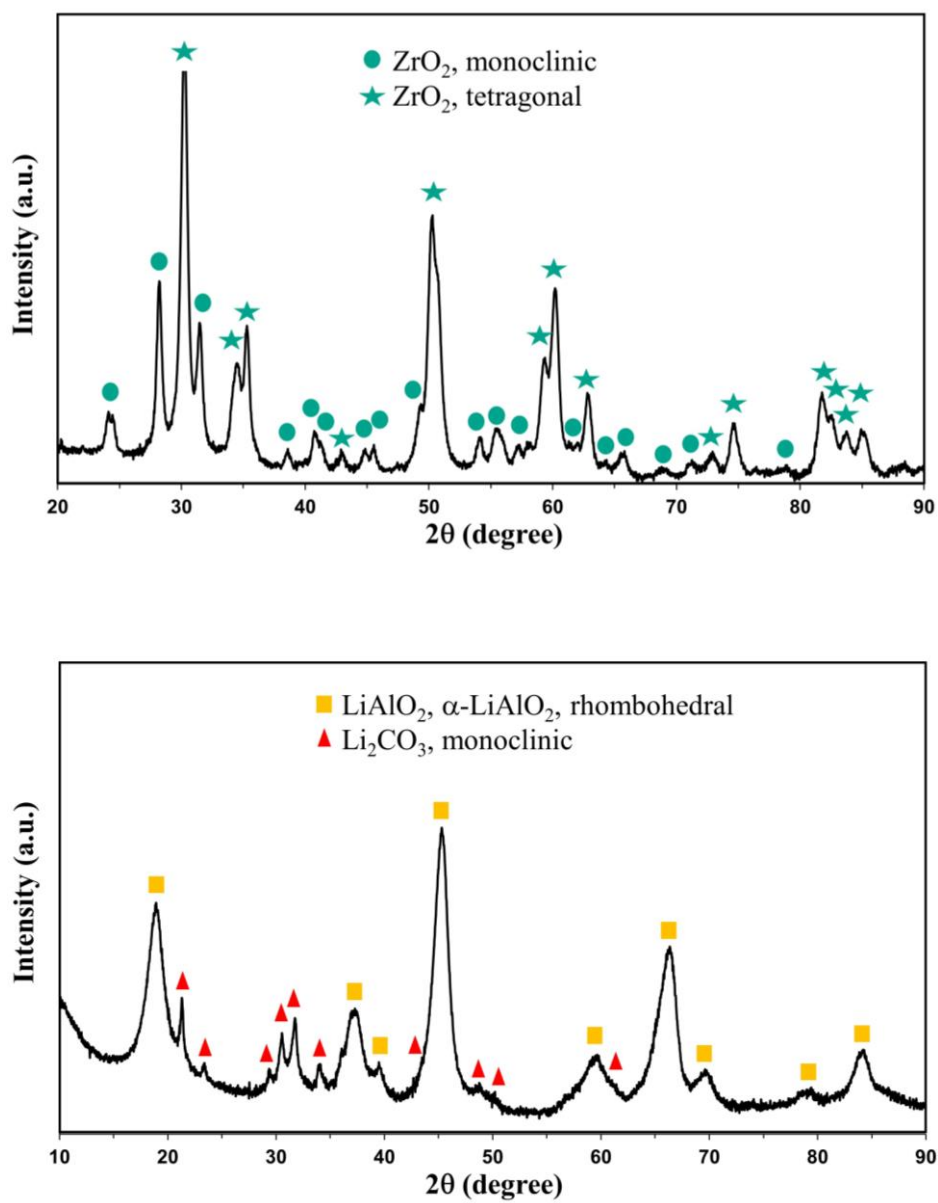


Figure S1. Continued.

Supporting Information

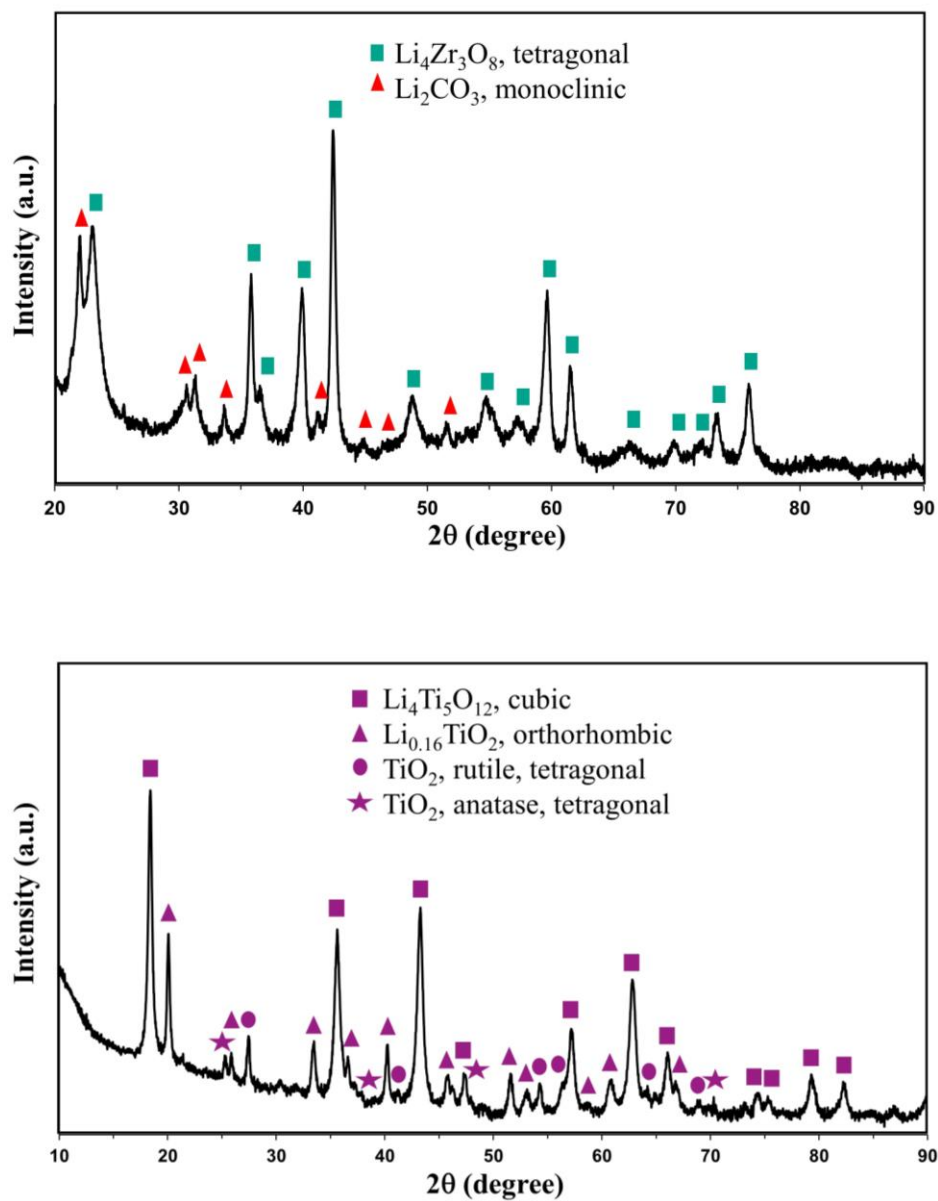


Figure S1. XRD patterns of fumed ZrO_2 , LiAlO_2 , $\text{Li}_4\text{Zr}_3\text{O}_8$, $\text{Li}_4\text{Ti}_5\text{O}_{12}$. Fumed ZrO_2 shows mostly tetragonal phase, LiAlO_2 shows the α -phase (rhombohedral), $\text{Li}_4\text{Zr}_3\text{O}_8$ is tetragonal and $\text{Li}_4\text{Ti}_5\text{O}_{12}$ has mostly a cubic structure.

Supporting Information

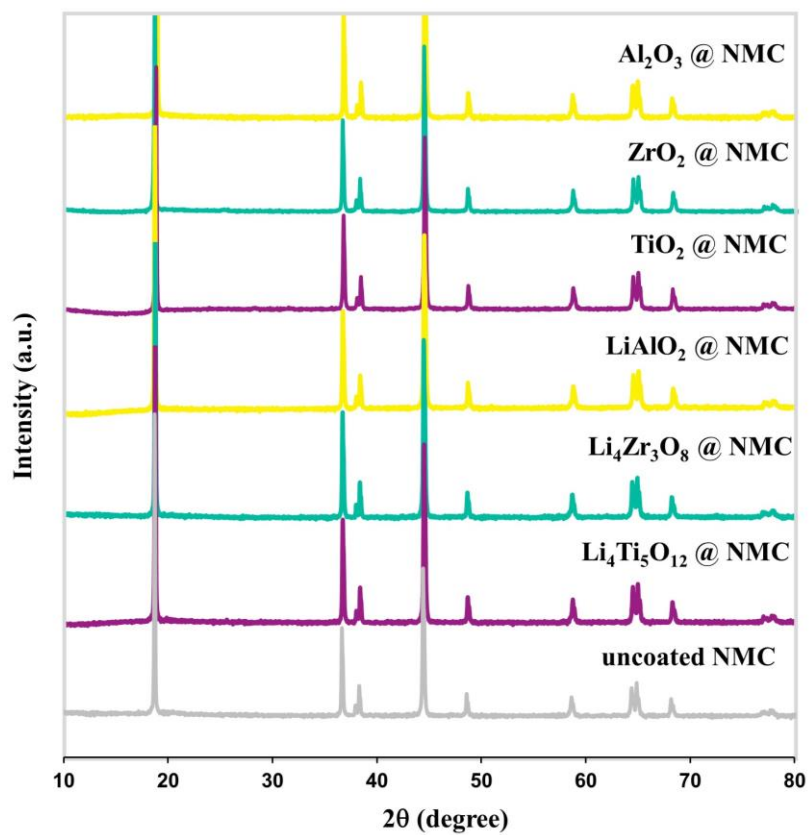


Figure S2. XRD patterns of NMC701515 coated by 1 wt % fumed Al_2O_3 , ZrO_2 , TiO_2 , LiAlO_2 , $\text{Li}_4\text{Zr}_3\text{O}_8$ and $\text{Li}_4\text{Ti}_5\text{O}_{12}$ compared to uncoated NMC.

Supporting Information

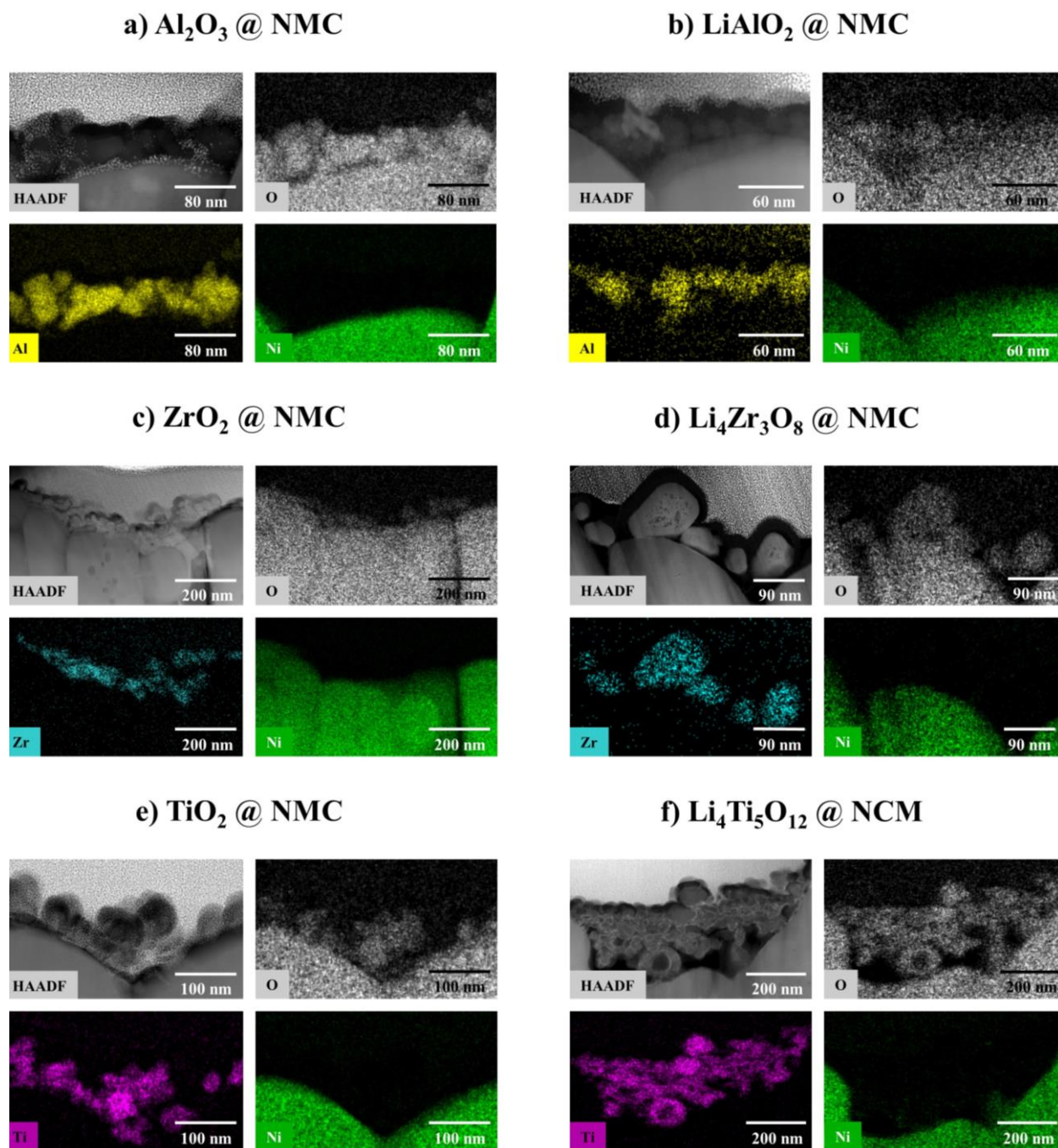


Figure S3. HAADF-STEM Z-contrast images and STEM-EDX analysis of cross-sections of NMC701515 coated with 1 wt % of the respective coating agent (a: Al_2O_3 , b: LiAlO_2 , c: ZrO_2 , d: $\text{Li}_4\text{Zr}_3\text{O}_8$, e: TiO_2 , f: $\text{Li}_4\text{Ti}_5\text{O}_{12}$). The distribution of nickel, manganese and cobalt is identical, therefore only the mapping of nickel is presented.

Supporting Information

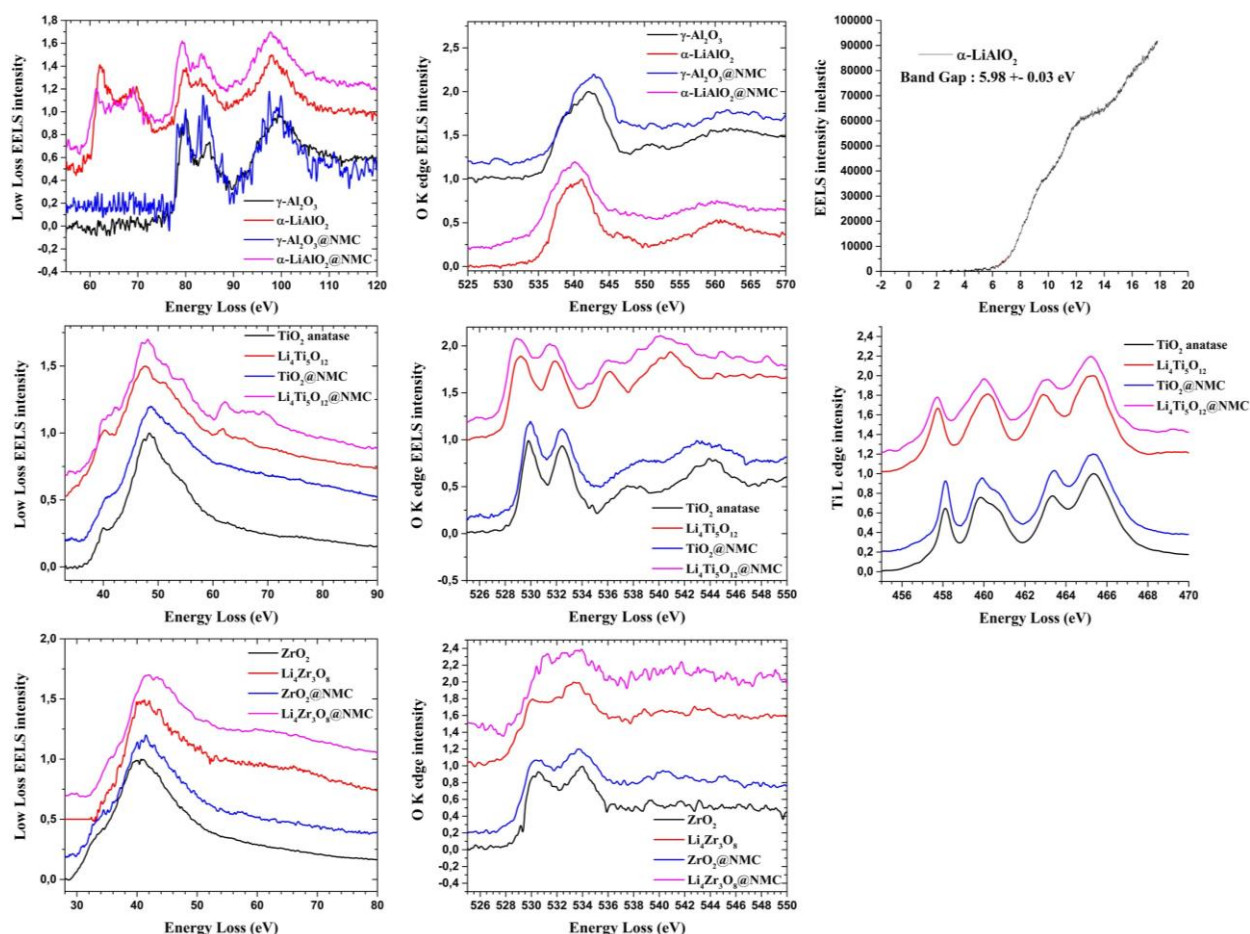


Figure S4. Electron energy-loss near edge structure (ELNES)-spectra/fine structures of the low loss regions and O K-edges of the respective coating materials, as well as the Ti L edge of the Ti-containing coating agents, before coating and after coating on high-nickel NMC. Comparison reveals that the chemical composition of the coating materials is not affected by the high-intensity dry coating process. These fine structures confirm the phases of the different coatings as anatase for TiO_2 , $\gamma\text{-Al}_2\text{O}_3$ and $\text{Li}_4\text{Ti}_5\text{O}_{12}$. The band gap determination of LiAlO_2 confirms the structure as $\alpha\text{-LiAlO}_2$.

Supporting Information

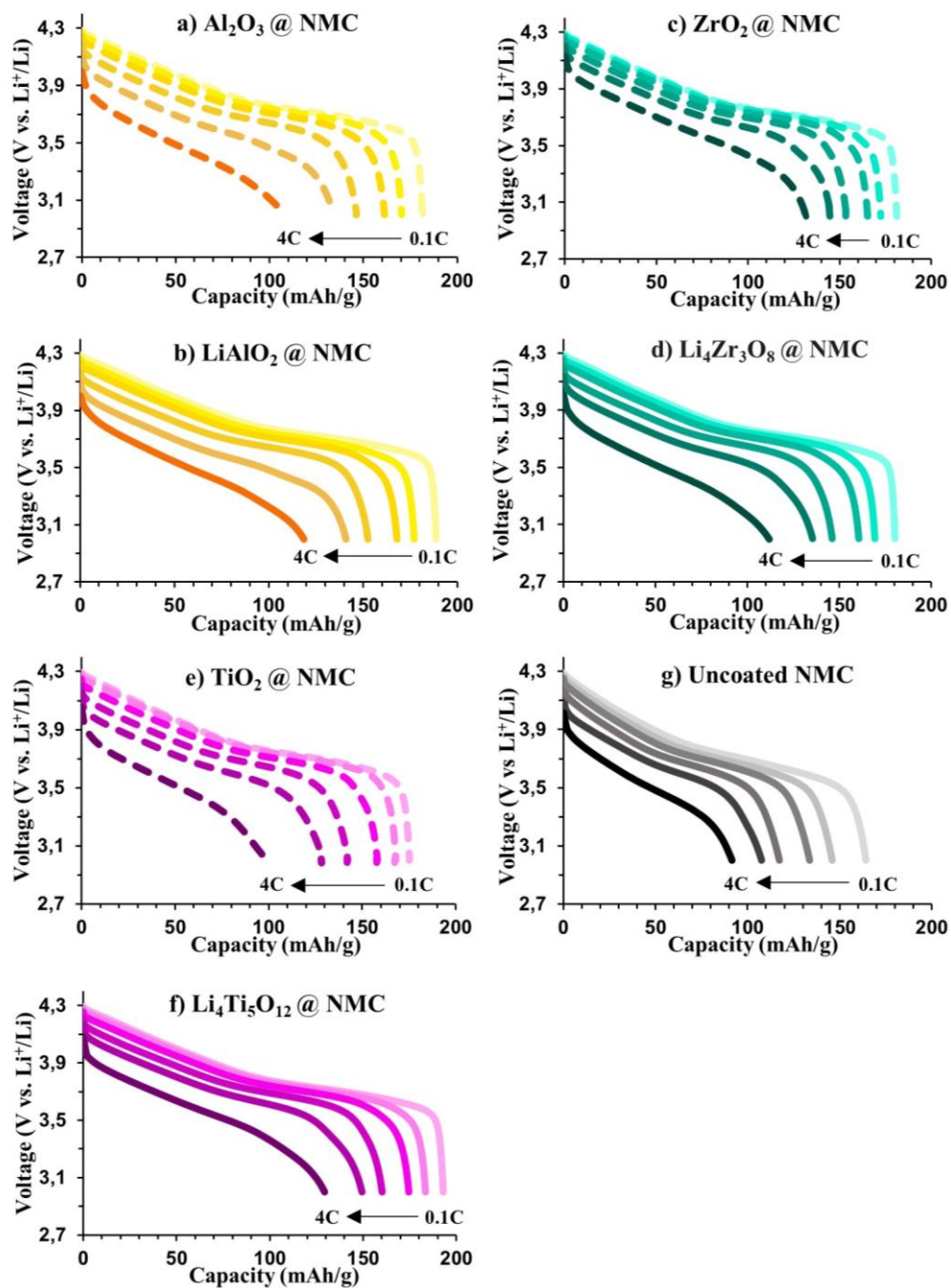


Figure S5. Galvanostatic discharge profiles of NMC coated with 1 wt % of the respective coating material (a: Al_2O_3 , b: LiAlO_2 , c: ZrO_2 , d: $\text{Li}_4\text{Zr}_3\text{O}_8$, e: TiO_2 , f: $\text{Li}_4\text{Ti}_5\text{O}_{12}$) and uncoated NMC (g) cycled between 3.0 – 4.3 V at room temperature at various discharge rates (C-rates).

Supporting Information

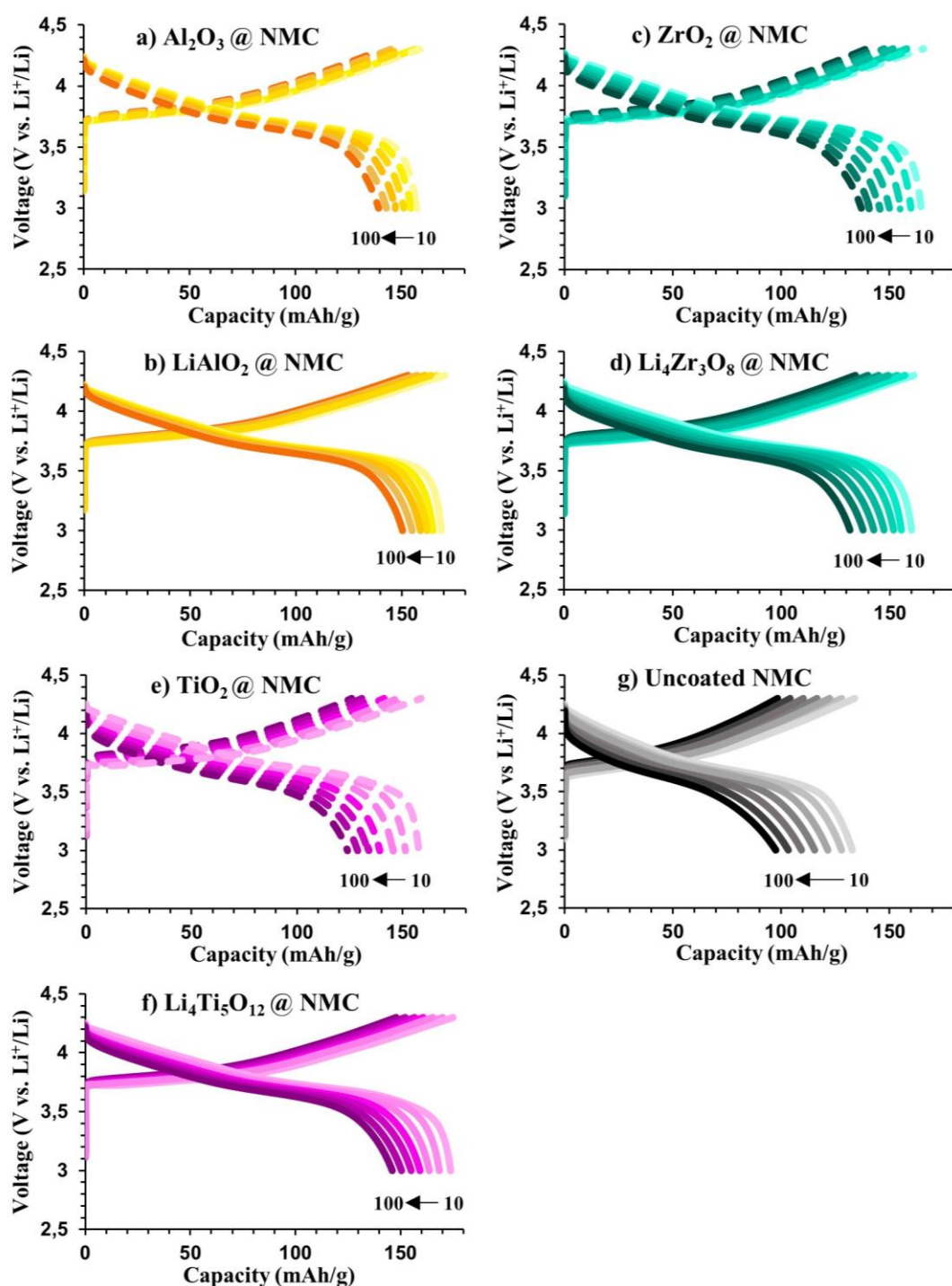


Figure S6. Galvanostatic charge and discharge profiles of the coated NMCs and uncoated NMC cycled between 3.0 – 4.3 V at room temperature (Discharge rate cycle 10-100: 0.5C, charge and discharge curves in steps of 15 cycles): a) Al_2O_3 , b) LiAlO_2 , c) ZrO_2 , d) $\text{Li}_4\text{Zr}_3\text{O}_8$, e) TiO_2 , f) $\text{Li}_4\text{Ti}_5\text{O}_{12}$ coated NMC and g) uncoated NMC.